Thermodynamics of small alkali halide cluster ions: comparison of classical molecular simulations with experiment and quantum chemistry

Lukas Vlcek,[*,1,2] *Filip Uhlik,*[3] *Filip Moucka,*[4] *Ivo Nezbeda,*[4,5] *and Ariel A. Chialvo*[1]

[1] Chemical Sciences Division, Geochemistry & Interfacial Sciences Group, Oak Ridge National Laboratory, Oak Ridge, TN 37831-6110, United States

[2] Joint Institute for Computational Sciences, Oak Ridge National Laboratory, Oak Ridge, TN 37831-6173, United States

[3] Department of Physical and Macromolecular Chemistry, Faculty of Science, Charles University, 128 43 Prague 2, Czech Republic

[4] Faculty of Science, J. E. Purkinje University, 400 96 Usti nad Labem, Czech Republic

[5] E. Hala Laboratory of Thermodynamics, Institute of Chemical Process Fundamentals, Academy of Sciences, 165 02 Prague 6, Czech Republic

Submitted to The Journal of Physical Chemistry A

Corresponding Author

*E-mail address: vlcekl1@ornl.gov

Abstract: We evaluate the ability of selected classical molecular models to describe the thermodynamic and structural aspects of gas-phase hydration of alkali halide ions and the formation of small water clusters. To understand the effect of many-body interactions (polarization) and charge penetration effects on the accuracy of a force field, we perform Monte Carlo simulations with three rigid water models using different functional forms to account for these effects: (i) point charge non-polarizable SPC/E, (ii) Drude point charge polarizable SWM4-DP, and (iii) Drude Gaussian charge polarizable BK3. Model predictions are compared with experimental Gibbs free energies and enthalpies of ion hydration, and with microscopic structural properties obtained from quantum DFT calculations. We find that all three models provide comparable predictions for pure water clusters and cation hydration, but differ significantly in their description of anion hydration. None of the investigated classical force fields can consistently and quantitatively reproduce the experimental gas phase hydration thermodynamics. The outcome of this study highlights the relation between the functional form that describes the effective intermolecular interactions and the accuracy of the resulting ion hydration properties.

Keywords: hydration properties, cluster-ion, molecular model, quantum chemistry, electro-spray mass spectrometry

1. Introduction

An accurate representation of ion hydration at low water densities is critical for the study of diverse atmospheric processes, such as cluster and droplet formation in ionosphere,[1] seawater sprays,[2] flames,[3,4] or electric discharges,[5] as well as for understanding the behavior of aqueous electrolytes in supercritical geochemical and industrial systems.[6,7] Beyond specific applications, small vapor-phase cluster ions offer a unique window into the fundamental problem of single-ion solvation thermodynamics because, unlike ions in bulk liquid solutions, individual cluster properties can be studied experimentally using mass spectrometric methods based on equilibrium measurements[8-14] and collision-induced dissociation.[15-17] The experimental results have been used as anchoring points for the extrapolation of hydration properties to bulk conditions,[18,19] as well as for the development and validation of classical molecular force fields.[20-25] The small size of cluster ions, typically comprising less than 10 water molecules, also provides a more direct insight into the specific details of ion-water interactions than bulk aqueous systems, thus, becoming a valuable source of information for force field optimization.

Computational studies of small gas-phase clusters have traditionally relied heavily on first principles quantum chemical approaches. Given the limited system sizes, accurate high-level quantum methods can be used to calculate the energies of selected cluster configurations[24] and lower-level DFT calculations can be used to collect samples from the first principles molecular dynamics (MD) or Monte Carlo (MC) simulations at finite temperatures.[26,27] At present, such simulations routinely cover MD trajectories spanning tens of picoseconds or generate thousands of MC cycles, which is sufficient for basic estimation of the cluster thermodynamics.[27] However, since accurate determination of thermodynamic properties (e.g., Gibbs free energy and entropy of hydration) requires much more extensive sampling of the system phase-space in the order of

tens of nanoseconds, which is not currently achievable by straightforward DFT-MD simulations, such calculations must be accomplished by either classical simulations or quantum/classical hybrid schemes.

Classical simulations of cluster ions have been used both to develop molecular models and to study ion hydration in vapor phases.[20-25] Perhaps the most common way cluster ions are used in force field development is as a reference for adjustment of interaction parameters to reproduce *ab initio* polymerization energies of selected locally optimized configurations. This approach, typically employed for polarizable models,[28-35] has also been used by Joung and Cheatham to develop their alkali-halide force fields compatible with non-polarizable models of water.[23] Although methodologically simple, the optimization based on minimum energy configurations may suffer from a bias resulting from overweighting more compact structures while underweighting a wide range of higher-energy structures that can contribute significantly to the cluster hydration entropy. This bias, however, can be avoided by using a larger number of canonically distributed cluster configurations obtained from MD or MC simulations at finite temperatures (usually at 298.15 K), while the model parameters can be then adjusted to reproduce experimental thermodynamic properties, trajectories from DFT-MD simulations, or both. This approach was used by Smith and Dang, who optimized their ion force-field parameters compatible with the polarizable water model (RPOL) to match incremental hydration enthalpies of Na^+ and Cl^- ions.[36] Likewise, Lamoreux and Roux adjusted the ion-water parameters based on their SWM4-DP model to reproduce the empirical enthalpies of ion monohydrates and found that the resulting model was able to predict reasonably well selected *ab initio* energies of larger clusters.[24] Moreover, Shevkunov used experimental cluster-ion thermodynamic properties to design a non-polarizable force field specifically for the description

of Cl^-water clusters, [37] while Lukyanov *et al*. performed an extensive systematic evaluation of the capability of a set of simple polarizable and non-polarizable models to predict cluster-ion binding hydration Gibbs free energies, enthalpies and entropies,[20] whose analysis has been recently extended by Zidi using a fluctuating charge polarizable model.[38] Finally, Grossfield et al. calculated the Cl^- cluster binding enthalpies for the flexible polarizable AMOEBA force field and found a close agreement with the high pressure mass spectrometry counterpart.[33]

While there have been numerous studies of small and medium size ion-water clusters addressing different challenges of the molecular based interpretation of ion hydration phenomena,[38-41] there is also an underlying interest in developing an accurate representation of ion-water clusters motivated by their key role in the determination of single-ion hydration properties.[18,42,43] However, as we argued in our recent study with non-polarizable models,[19] and supported by simulations with the more sophisticated polarizable AMOEBA model,[44] the current extrapolations from clusters to bulk hydration rely on unjustified assumptions. A direct path to more accurate determination of single-ion thermodynamics is to span the experimentally inaccessible cluster-to-bulk transition using highly accurate molecular models. In the present study we investigate the ability of three currently available classical rigid models (and corresponding force field parameterizations) to describe the properties of small ion-water clusters as determined by macroscopic thermodynamic experiments and microscopic quantum mechanical simulations. These models are characterized by contrasting approaches used to account for polarization effects that range from pair-wise effective polarizable contributions using fixed-charge electrostatics, to multi-body induced polarization via molecular Drude point charges (one per H_2O),[24] and finally to polarization described by atomic Drude oscillators with Gaussian charges (three per H_2O).[28] The analysis of model behavior across large data sets can

reveal trends that would not be apparent from isolated data points and identify essential interactions needed for reliable description of ion hydration. The outcome of this comparison should provide guidance for the future development of highly accurate potential models to facilitate large-scale simulations of aqueous ions in both vapor and liquid phases over a wide range of thermodynamic conditions and environments. Even though we employ a simple flexible model of water in our hybrid classical-quantum DFT Monte Carlo scheme, we defer a more comprehensive analysis of the role of flexibility and other features to future studies.

The remainder of the article is organized as follows: In Section 2 we define the essential concepts and models needed for the study of cluster ions, and describe our computational methodology; in Section 3 we present structural and thermodynamic results pertaining to cluster-ions and discuss the performance of different force fields; in Section 4 we summarize our findings and highlight their implications in the development of more accurate aqueous electrolyte interaction models.

2. Theoretical background

2.1.Basic relations

The thermodynamics of gas-phase ion hydration and formation of cluster ions at finite temperatures and pressures is typically expressed in terms of elementary stepwise (or incremental) reactions and their associated enthalpies and Gibbs free energies.

The standard state (*i.e.*, T° = 298.15 K and P° = 1 bar) enthalpy, $\Delta H^\circ_{n-1,n}[A]$, and Gibbs free energy, $\Delta G^\circ_{n-1,n}[A]$, of a stepwise hydration reaction,

$$A(H_2O)_{n-1} + H_2O \rightarrow A(H_2O)_n \ , \tag{1}$$

in which a cluster-ion comprising an ion *A* and *n-1* water molecules binds an additional water molecule, can be expressed as follows,

$$\Delta H^{\circ}_{n-1,n}\left[A\right] = H^{\circ}\left[A\left(\mathrm{H_2O}\right)_n\right] - H^{\circ}\left[A\left(\mathrm{H_2O}\right)_{n-1}\right] - H^{\circ}\left[\mathrm{H_2O}\right] \quad (2a)$$

$$\Delta G^{\circ}_{n-1,n}\left[A\right] = G^{\circ}\left[A\left(\mathrm{H_2O}\right)_n\right] - G^{\circ}\left[A\left(\mathrm{H_2O}\right)_{n-1}\right] - G^{\circ}\left[\mathrm{H_2O}\right] \quad (2b)$$

The thermodynamic quantities listed on the right-hand side of Eqs. (2) correspond to individual reactants and products (*i.e.*, cluster-ions comprising *n* and *n-1* water molecules, and a single water molecule, respectively) in the ideal gas state at standard conditions. The enthalpies of reactants and products appearing in Eq. (2a) can be decomposed into the following components,

$$H^{\circ} = K^{\circ} + U + P^{\circ}V \quad (3)$$

where K° and *U* are the average kinetic and potential energies, *V* is the molar volume of the species at the standard pressure P°. Since the interparticle potential energy of an isolated water molecule is zero it results that, to determine $\Delta H^{\circ}_{n-1,n}\left[A\right]$, it suffices to calculate the difference between the enthalpies of cluster-ions comprising *n* and *n-1* water molecules followed by the subtraction of the ideal gas enthalpy contribution of classical rigid water molecules (3*RT* for translational and rotational degrees of freedom and 1*RT* for the *PV* term of ideal gas) at the standard temperature T°, i.e.,

$$\Delta H^{\circ}_{n-1,n}\left[A\right] = H^{\circ}\left[A\left(\mathrm{H_2O}\right)_n\right] - H^{\circ}\left[A\left(\mathrm{H_2O}\right)_{n-1}\right] - 4RT^{\circ} \ . \quad (4)$$

The difference of Gibbs free energy between clusters comprising *n* and *n-1* water molecules, i.e., the first two terms in the right-hand-side of Eq. (2b), can be extracted from the grand canonical probability $p_i(n)$ of finding a cluster-ion with *n* water molecules in a system characterized by the chemical potential of water, $\mu_i(T,V)$, defined as

$$p_i(n) = \frac{Q(n)\exp[\beta\mu_i n]}{\exp[-\beta\Omega_i]} \qquad (5)$$

where Ω_i is the classical bulk grand potential ($\Omega_i = -P_i V$) and $Q(n)$ is the canonical partition function of a system with one ion and n water molecules within volume V, at temperature T, where $\beta = 1/k_B T$, and k_B is the Boltzmann constant. The probability $p_i(n)$ can be calculated using grand canonical Monte Carlo (GCMC) simulations from a normalized histogram,

$$p_i(n) = \frac{\mathcal{H}_i(n)}{\mathcal{H}_i^{TOT}} \qquad (6)$$

where $\mathcal{H}_i(n)$ denotes the histogram count for clusters with n water molecules and $\mathcal{H}_i^{\mathrm{TOT}}$ is the total number of cluster-size measurements. Since the ideal gas $P^\circ V$ contributions from the two cluster-ions cancel out, the difference of Gibbs free energies in Eq. (2b) can be equated to the corresponding difference of Helmholtz free energies $\Delta F(n,n-1)$ which, according to Eqs. (5) and (6), can be expressed as,

$$\beta\left\{F\left[A(\mathrm{H_2O})_n\right] - F\left[A(\mathrm{H_2O})_{n-1}\right]\right\} = -\ln\left[\frac{Q(n)}{Q(n-1)}\right] = -\ln\left[\frac{\mathcal{H}_i(n)}{\mathcal{H}_i(n-1)}\right] + \beta\mu_i \quad . \qquad (7)$$

Equation (7) suggests that, from a simulation standpoint, a series of GCMC simulations of clusters at different values of $\mu_i(T,V)$ can be seamlessly combined using the histogram reweighting technique.[19,45] Subsequently, the stepwise Gibbs free energy difference defined in Eq. (2b) can be finally calculated as follows,

$$\Delta G^\circ_{n-1,n}[A] = F\left[A(\mathrm{H_2O})_n\right] - F\left[A(\mathrm{H_2O})_{n-1}\right] - \mu^{\circ,ig}[\mathrm{H_2O}] \qquad (8)$$

where $\mu^{\circ,ig}\left[\mathrm{H_2O}\right]$ is the chemical potential of isolated (ideal gas) water molecules at the standard conditions (P°, T°).

In the case of small pure-water clusters, whose instability results in poor GCMC sampling, the free energy difference between clusters comprised of *n* and *n-1* water molecules, $\Delta F(n,n-1)$, can be determined more efficiently using Bennett's acceptance ratio (BAR) method,[46] which permits a more flexible and focused sampling of the configurational space. To apply this approach to the hydration reaction of Eq. (1) the reaction path must be split into two steps: (i) add a non-interacting water molecule to a cluster with *n-1* water molecules, followed by (ii) switch on the interactions of the new molecule with the rest of the system, i.e.,

$$\beta\left\{F\left[A\left(\mathrm{H_2O}\right)_n\right]-F\left[A\left(\mathrm{H_2O}\right)_{n-1}\right]\right\}=-\ln\left[\frac{Q_0(n)}{Q(n-1)}\right]-\ln\left[\frac{Q(n)}{Q_0(n)}\right], \qquad (9)$$

where $Q_0(n)$ denotes the canonical partition function of a cluster-ion with one non-interacting and *n-1* interacting water molecules. The first term on the right-hand side of Eq. (9) corresponds to the Helmholtz free energy of a non-interacting water molecule moving within the volume of a cluster comprising *n* water molecules, i.e.,

$$\frac{Q_0(n)}{Q(n-1)}=\frac{V}{nq^{iso}} \qquad (10)$$

where q^{iso} stands for the product of the translational, rotational, vibrational, and electronic partition functions of an isolated water molecule.[47] The second term on the right-hand side of Eq. (9) corresponds to the free energy change caused by the switch on of the interactions of the extra particle whose contribution can be determined using Widom's test particle method[48] during a canonical MC or MD simulations of a cluster with *n-1* water molecules, i.e.,

$$\frac{Q(n)}{Q_0(n)}=\left\langle\exp\left[-\beta\left(u-u_0\right)\right]\right\rangle_0 . \qquad (11)$$

Here u and u_0 are the energies of the same configuration in the systems with n and $n-1$ fully interacting water molecules and $\langle \ldots \rangle_0$ denotes averaging over equilibrium configurations of the system with one non-interacting molecule. However, to reduce any bias that can be introduced by the test particle method when extensive sampling is not available, we use the BAR method, which combines samples taken from the two systems characterized by $Q(n)$ and $Q_0(n)$, i.e.,

$$\frac{Q(n)}{Q_0(n)} = \frac{\langle w \exp[-\beta u] \rangle_0}{\langle w \exp[-\beta u_0] \rangle} . \qquad (12)$$

where w is a properly chosen weighting function.[46] Since the non-interacting particle can easily sample configurations present in the fully-interacting system, there is enough overlap between configurations of $Q(n)$ and $Q_0(n)$, and the outcome of Eq. (12) should not be significantly biased. The variance (i.e., as a measure of the statistical error) of the calculated free energy averages can be reduced by a judicious adjustment of the relative number of samples taken from the two systems. As a test of correctness of our BAR and GCMC implementations, we have confirmed that both methods yield the same cluster-ion $\Delta F(n,n-1)$ values.

2.2. Definition of a cluster

The analysis of cluster-ion properties and their comparison with the corresponding experimental data requires a definition of what constitutes a cluster that is compatible with the experimental setup. Since most ion-water and water-water clusters at finite temperatures are transient structures, any criterion used for their definitions must select structures stable enough to undergo the experimental measurement.

Perhaps the most sophisticated cluster definitions are based on kinetic considerations of cluster stability derived from the rate of evaporation, which have been used to study a water

dimer.[49] Unfortunately, this approach is not practical for the present study that involves millions of possible configurations of up to 7 particles. Other definitions involve geometrical criteria based on particle-pair connectivity,[50] as well as distance-based criteria specifically designed to deal with cluster-ions.[51] While simple in specific cases, geometrical criteria are difficult to generalize for more complex systems containing mixtures of molecular particles, such as in the present study that requires consistent treatment of cluster ions and pure water clusters. Instead here we opt for two energy-based stability criteria, A and B, similar to those proposed by Hill[52,53] and used for simple and fast identification of clusters.[54,55] Neither of our criteria will result in the selection of indefinitely stable clusters, with the exception of a dimer of structureless atomic particles. According to criterion A, a stable dimer is formed when the pair interaction energy is lower than the mutual kinetic energy, i.e.,

$$u_{ij}\left(\mathbf{r}_i,\mathbf{r}_j\right) \le -\left(\mathbf{p}_i-\mathbf{p}_j\right)^2 \Big/ 4\mu \ . \tag{13}$$

Here i and j represent two particles or groups of particles whose mutual interaction energy is u_{ij}, $\mathbf{r}_i$ and $\mathbf{p}_i$ are the vector position and linear momentum of i, respectively, while μ is the reduced mass of the binary system. Therefore, relation (13) selects a subset of particles within the multidimensional configurational and momentum space. Unlike the original work by Hill, which dealt with pairwise additive interactions and resulted in a definition based on pairwise connectivity, our study considers many-body interactions and the cluster definition must be modified accordingly.

Here we consider a configuration of N particles that would form a cluster when the interaction energy of any subset of the N particles with the remainder of the system satisfies the condition given by Eq. (13). When the cluster analysis is performed during MC simulations, all

particles are assigned random momentum vectors, $\mathbf{p}_i$, from the Gaussian distribution consistent with the external temperature, and then the condition (13) is evaluated.

We have also used an alternative simplified criterion (B) based only on configurational energies. It is equivalent to A with the assumption that all particles and their groups have the average translational kinetic energy of 3/2 k_BT. Accordingly, Eq. (13) reduces to:

$$u_{ij}\left(\mathbf{r}_i,\mathbf{r}_j\right) \le -3/2\, k_B T \qquad (14)$$

Since this simplified criterion selects a subset of the configurational space but considers the full momentum space, the kinetic energies of the reactants and products are the same, and consequently Eq. (4) becomes,

$$\Delta H^{\circ}_{n-1,n}[A] = U\left[A\left(\mathrm{H_2O}\right)_n\right] - U\left[A\left(\mathrm{H_2O}\right)_{n-1}\right] - RT^{\circ}.$$

For cluster ions at 298.15 K, this criterion corresponds roughly to the average ion-water interaction energy at a distance of 10 Å from the central ion, which is the diameter of the cluster-containing cavity used by Lukyanov et al.[51] Results based on our energetic criterion B will therefore correspond closely to those that would be obtained according to this geometric definition.

2.3.Classical models of aqueous electrolytes

2.3.1. Non-polarizable model based on the SPC/E water

The simplest force field considered in this study is represented by a rigid non-polarizable interaction-site model of water and ions, in which the functional form of the site-site potential combines Lennard-Jones (LJ) and point charge interactions, *i.e.*,

$$U_{IW}\left(\mathbf{r}_{IW}\right)=\sum_{j=1}^{N}4\varepsilon_{IO}\left[\left(\frac{\sigma_{IO}}{\left|\mathbf{r}_I-\mathbf{r}_{jO}\right|}\right)^{12}-\left(\frac{\sigma_{IO}}{\left|\mathbf{r}_I-\mathbf{r}_{jO}\right|}\right)^{6}\right]+\sum_{j=1}^{N}\sum_{s=1}^{S}\frac{q_I q_s}{\left|\mathbf{r}_I-\mathbf{r}_{js}\right|} \quad (15)$$

Here $U_{IW}\left(\mathbf{r}_{IW}\right)$ is the energy of interaction between ion *I* and surrounding *N* water molecules; ε_{IO} and σ_{IO} are the Lennard-Jones energy and size parameters of the ion-water oxygen, *IO*, interaction; q_I and q_s are charges on ion *I* and site *s* of a water molecule, respectively; expression $\left|\mathbf{r}_I-\mathbf{r}_{js}\right|$ denotes the distance between ion *I* and site *s* on water molecule *j*. The model was developed by Joung and Cheatham[23] for use with the SPC/E water[56] with the ion-water force field parameters optimized against multiple experimental properties including ion radii, hydration free energies at infinite dilution, crystal geometry and lattice energy, as well as *ab* initio-derived energies of selected cluster configurations. The resulting parameters are summarized in Table S1 (Supplementary Information). This force field has been used earlier to study the adequacy of the cluster-pair based approximation, for which only relative cation-anion thermodynamics was required.[19] In contrast, here we use them to calculate the absolute values of the corresponding quantities.

2.3.2. Polarizable model based on the SWM4-DP water

The SWM4-DP model shares the Lennard-Jones and point charge functional form with the SPC/E-based model, Eq. (15), but adds polarizable interaction on the oxygen site through the Drude charge-on-spring scheme.[57] The interactions between an ion and *N* water molecules are defined by the following expression:

$$U_{IW}(\mathbf{r}_{IW}) = \sum_{j=1}^{N} 4\varepsilon_{IO}\left[\left(\frac{\sigma_{IO}}{|\mathbf{r}_I - \mathbf{r}_{jO}|}\right)^{12} - \left(\frac{\sigma_{IO}}{|\mathbf{r}_I - \mathbf{r}_{jO}|}\right)^{6}\right] + \sum_{j=1}^{N}\sum_{s=1}^{S}\left[\frac{(q_I - \delta q)q_s}{|\mathbf{r}_I - \mathbf{r}_{js}|} + \frac{\delta q q_s}{|\mathbf{r}_D - \mathbf{r}_{js}|}\right] + \frac{1}{2}k_D|\mathbf{r}_I - \mathbf{r}_D|^2 \quad . \qquad (16)$$

Here δq is the charge of the Drude particle D, $\mathbf{r}_D$ is its vector position, and k_D is the force constant of the harmonic potential between the ion I and the particle D, where the remaining symbols have the same meaning as in Eq. (15). The model was optimized using scaled *ab initio*-based polarizabilities, binding energies of ion-water dimers at 298.15 K, and bulk hydration free energies of neutral ion pairs.[24] The resulting parameters are summarized in Table S1.

2.3.3. Polarizable model based on the BK3 water

The BK3 model uses Gaussian charges to represent the Coulombic interactions and the Buckingham (exponential-6) potential to describe the non-Coulombic interactions, while the polarizability of the water molecule is implemented through three Drude particle-on-spring sites located at the oxygen and two hydrogen atoms so that the ion-water interaction energy can be written as follows,[28,58]

$$U_{IW}(\mathbf{r}_{IW}) = \sum_{j=1}^{N}\left[A_{IO}\exp\left(-B_{IO}|\mathbf{r}_I - \mathbf{r}_{jO}|\right) - \frac{C_{IO}}{|\mathbf{r}_I - \mathbf{r}_{jO}|^6}\right] + \sum_{j=1}^{N}\sum_{s=1}^{S}\left[\frac{(q_I - \delta q)q_s}{|\mathbf{r}_I - \mathbf{r}_{js}|}\mathrm{erf}\left(|\mathbf{r}_I - \mathbf{r}_{js}|\gamma_{Ij}\right) + \frac{\delta q q_s}{|\mathbf{r}_D - \mathbf{r}_{js}|}\mathrm{erf}\left(|\mathbf{r}_D - \mathbf{r}_{js}|\gamma_{Ij}\right)\right] + \frac{1}{2}k_D|\mathbf{r}_I - \mathbf{r}_D|^2 \qquad (17)$$

Here A_{IO}, B_{IO}, and C_{IO} are the parameters of the Buckingham potential between the ion *I* and the water oxygen *O*; $\gamma_{Is} = \sqrt{\gamma_I \gamma_s}$, with γ_I and γ_s being the width of the Gaussian charges on ion *I* and water site *s*, respectively, and the remaining symbols have the same meaning as in Eq. (16). The entire set of BK3 parameters is summarized in Table S1. The model was optimized to reproduce experimental hydration free energies of neutral alkali halide salts in infinitely diluted bulk solutions and to maintain the hydration free energy differences within the same-charge series of alkali metal and halide ions.

2.4. Classical Monte Carlo simulations

The microstructural properties and enthalpies of ion hydration involving clusters with n = 1 to 6 water molecules were calculated from the isochoric-isothermal Monte Carlo (NVT-MC). The hydration Helmholtz free energies were calculated from a series of GCMC[59] simulations in which the water chemical potential, μ_t(T,V), was fixed at different values (corresponding to the changing water vapor pressure in the experiment) and the statistics of cluster sizes was analyzed using the histogram reweighting technique[45] as described elsewhere.[19] Additionally, the Helmholtz free energies were also calculated from trial water molecule insertions and deletions performed during the NVT-MC runs.

All simulations were performed in a 28 x 28 x 28 Å box at 298.15 K, where the particle interactions were truncated at a cutoff distance of 12 Å, which is sufficient to minimize errors from incorrectly excluding clusters based on our definitions A and B (see Section 2.2). The length of NVT-MC simulations exceeded 1×10^8 individual translational and rotational MC steps, and the combined length of the GCMC simulations for each ion was at least 1×10^9 individual translational, rotational, and insertion/deletion MC steps, where the translations and rotations

were accomplished with multi-particle moves.[60] Both the MC simulations and histogram reweighting were performed using in-house codes.

Before proceeding we need to provide the following details on the calculation of $\Delta F(n,n-1)$: In equations (5) to (7) we assumed that the cluster occupies the full phase space available to an ion and *n* water molecules in the volume V. However, to account for the definition of a cluster as occupying only a subset of the full phase space (see Section 2.2), we have to modify the equations for the probability of a cluster formation to satisfy our definitions A and B. The partition function and the histogram can be separated into cluster and non-cluster parts as follows:

$$\begin{aligned} Q(n) &= Q_{c}(n) + Q_{\bar{c}}(n) = Q_{c}(n)\left(1 + \frac{Q_{\bar{c}}(n)}{Q_{c}(n)}\right) \\ \mathcal{H}_{i}(n) &= \mathcal{H}_{c,i}(n) + \mathcal{H}_{\bar{c},i}(n) = \mathcal{H}_{c,i}(n)\left(1 + \frac{\mathcal{H}_{\bar{c},i}(n)}{\mathcal{H}_{c,i}(n)}\right), \end{aligned} \tag{18}$$

where the subscript c denotes the part of the canonical partition function pertaining to clusters and $\bar{c}$ denotes its complement. Equation (7) can then be re-written as follows:

$$\begin{aligned} &\beta\left\{F_{c}\left[A(\mathrm{H_2O})_{n}\right] - F_{c}\left[A(\mathrm{H_2O})_{n-1}\right]\right\} = -\ln\left[\frac{\mathcal{H}_{c,i}(n)}{\mathcal{H}_{c,i}(n-1)}\right] + \beta\mu_{i} \\ &= \beta\left\{F\left[A(\mathrm{H_2O})_{n}\right] - F\left[A(\mathrm{H_2O})_{n-1}\right]\right\} + \ln\left[\frac{1+\mathcal{X}(n)}{1+\mathcal{X}(n-1)}\right] \end{aligned} \tag{19}$$

where $\mathcal{X}(n) = \mathcal{H}_{\bar{c}}(n)/\mathcal{H}_{c}(n)$ is the ratio of non-clusters to clusters in a simulation box with *n* water molecules, which can be obtained both from NVT-MC or GCMC simulations.

2.5. Ab initio simulations

The microstructural properties of small ion-water clusters can be efficiently studied by simulations in which the particle interactions are determined using quantum chemical methods. Although the present simulations do not explicitly take into account purely quantum effects, such as the zero-point energy or proton tunneling, it has been shown that the structural features, such including the peak positions of radial distribution functions analyzed in the present study, are rather insensitive to them.[61]

The cluster-ions were studied using NVT-MC simulations with potential energies determined from the quantum density functional theory (DFT). In particular, a hybrid generalized-gradient approximation (GGA) density functional ω-B97X-D with long-range dispersion corrections[62] was used since it was found to accurately reproduce the results of higher-level *ab initio* methods for water clusters.[63] Dunning's correlation-consistent basis sets of double-zeta quality augmented with diffuse functions were used for that purpose.[64] All calculations were performed using Gaussian 09 program package[65] implemented as a back-end for a nested Monte Carlo simulation program.[66] Computationally inexpensive flexible empirical potentials[67,68] in the inner part were subsequently corrected by accurate but computationally expensive DFT potential energies in the outer part. The magnitude and number of inner Monte Carlo steps were tuned to keep reasonably high the corresponding acceptance probabilities. The initial parts of simulations were discarded and the simulations were run until several thousands of independent samples of cluster configurations were accumulated.

3. Results and Discussion

3.1. Pure water clusters

Before analyzing cluster-ion properties, it is helpful to assess the ability of molecular models to describe water-water interactions in pure water clusters. For that purpose we illustrate in Figure 1 the evolution of the calculated incremental hydration free energies and enthalpies of water at 298.15 K, which are also listed in Table S2 in the Supporting Information document. We note that the experimentally based estimates of properties of water clusters derived from thermodynamic considerations and virial coefficients[18,69-72] cannot be directly compared with the clusters based on the present definitions, which, unlike the experimental estimates, assume zero cluster-cluster interactions in water vapor (e.g., see related discussion by Hill[52]). Nevertheless, as a reference, we display the experimental estimates along with our results, and also include values from quantum chemical calculations taken from the available literature.[73]

As a first step, we analyzed the effect of the cluster definition (see Section 2.2) on the calculated thermodynamic properties. The resulting properties according to both cluster definitions (listed in Tables S2a and S2b) differ from each other by less than 1 kJ/mol, a difference significantly smaller than the absolute values of $\Delta G^{\circ}_{n-1,n}$ and $\Delta H^{\circ}_{n-1,n}$. Consequently, following qualitative discussion can be considered valid for either cluster definition.

In Figure 1 we plot the resulting incremental hydration Gibbs free energies and enthalpies of water clusters from the three water models against *ab initio* calculations, where we can highlight several features. The $\Delta G^{\circ}_{n-1,n}$ and $\Delta H^{\circ}_{n-1,n}$ values predicted by the non-polarizable SPC/E model are consistently more negative than those predicted by the polarizable models. However, note that this direct comparison does not take into account the self-polarization correction of ~5.23 kJ/mol built into the model, which represents the intramolecular energy needed to increase the water dipole moment from its vacuum value (1.85 D) to that of the SPC/E model (2.35 D).[56] Since the SWM4-DP and BK3 models include this contribution in the total thermodynamic

properties, it should also be added to the SPC/E results in order to make consistent comparisons. After the correction, the SPC/E results are in close agreement with the polarizable models; in fact, the agreement between the corrected SPC/E and BK3 predictions of $\Delta G^{\circ}_{n-1,n}$ is better than that between the two polarizable models. It is somewhat surprising that a model as simple as the SPC/E can describe gas phase water interactions so close to much more complex force fields. This observation may indicate that short-range hydrogen bond interactions (as opposed to longer-range dipolar interactions) are the dominant contributor to cluster thermodynamics with similar strength in the gas and liquid phases. The agreement between *ab initio* calculations and SPC/E simulated $\Delta G^{\circ}_{n-1,n}$ along with a more negative deviation for $\Delta H^{\circ}_{n-1,n}$ suggests more localized hydrogen bonds resulting in structures characterized by low energy and low entropy (see Table S2). However, despite the favorable predictions of the SPC/E model, we cannot generalize these observations to other empirical force fields, whose cluster property predictions can differ qualitatively.[74]

Another notable trend present in Figure 1 is the significant difference between the quantum chemical and classical model predictions showing up for the $\Delta G^{\circ}_{n-1,n}$, despite the close agreement of $\Delta H^{\circ}_{n-1,n}$. We believe that the reason for the discrepancy lies in the 'Boltzmann averaging over low energy structures', as described in the original literature,[73] that leads to underestimation of higher energy configurations, which contribute more significantly to the system's entropy.

A distinctive feature of all classical simulation results in Figure 1 is the presence of a minimum in the size dependence of the cluster properties corresponding to tetramer clusters. Further analysis of the results and comparison with quantum chemical studies in the literature[73] suggests that mechanism underlying this minimum is the formation of remarkably stable cyclical configurations. These configurations can be also identified through the presence of the next-

nearest neighbor peak at 4 Å in the plot of oxygen-oxygen pair distribution functions for $n = 4$ as illustrated in Figure 2. The minimum appears more pronounced for $\Delta H^{\circ}_{n-1,n}$ than for $\Delta G^{\circ}_{n-1,n}$ indicating an underlying trade-off between energetic favorability of the ring structures and their unfavorably low entropy. Incorporation of an additional water molecule ($n = 5$) to the cluster will result in a more loosely bound structure as evidenced by the lower incremental enthalpy and the wide second peak in Figure 2.

3.2. Ion-water clusters

To evaluate the uncertainty associated with the cluster definition, we have calculated the cluster-ion thermodynamics based on our two criteria, A and B (see Section 2.2). The resulting two sets of $\Delta G^{\circ}_{n-1,n}$ and $\Delta H^{\circ}_{n-1,n}$ listed in Table S3 differ by less then 0.01 kJ/mol, which is less than the statistical uncertainty associated with the simulated quantities. Therefore, for all practical purposes, the following discussion can be considered valid for either cluster definition. Only a small fraction (0 – 2 %) of the generated configurations was classified as non-clusters, which shows the large stability of the systems where all water molecules are contained within the deep Coulombic potential well of the central ion and forming its first hydration shell. The observed stability also reduces the uncertainty about the proper cluster definition.

The hydration structure and thermodynamics of cations and anions differ qualitatively as a result of water molecule asymmetry, and these differences persist over clusters of all sizes.[19] The main contribution to ion hydration energies in the small clusters investigated here comes from contact interactions in the first hydration shell. For cations, the dominant attractive term is the Coulombic interaction with water oxygens, while for anions, it comes from strong hydrogen

bonding that involves purely quantum mechanical effects,[75] and whose proper description is often difficult even with more sophisticated classical force fields.

The plots of cationic $\Delta G^{\circ}_{n-1,n}$ in Figure 3 show that the overall agreement of the two polarizable models with the high pressure mass spectrometry (HPMS) experimental data of Dzidic and Kebarle[13] is nearly quantitative for most ions, whereas the non-polarizable model predictions are consistently shifted to more negative values. As in the case of pure water clusters, most of the shift can be explained by the SPC/E self-polarization correction. In the case of larger cations (i.e., K^+ and Rb^+), the corrected SPC/E values are in close agreement with the predictions of the polarizable models over the full range of cluster sizes. Even in the case of the smallest Li^+ ion, for which the largest induced water dipoles are detected, the corrected non-polarizable predictions do not significantly deviate from the behavior of more complex force fields. The large constant deviation of the Cs^+ values seems to be caused by the particular choice of the LJ parameters rather than a failure of the non-polarizable representation. Indeed, the LJ parameters of the $Cs^+ - H_2O$ interaction deviate strongly from the trend established by smaller cations (see Table S1), which may indicate difficulties in their optimization that aimed to reproduce not only aqueous solution properties but also those of alkali halide crystals.[23]

The trends seen for cationic $\Delta G^{\circ}_{n-1,n}$ are reproduced and magnified in the plots of $\Delta H^{\circ}_{n-1,n}$ in Figure 4. There is very little difference between the predictions of the two polarizable models despite their contrasting functional descriptions of the Coulombic and non-Coulombic interactions, including the polarization sites. The corrected SPC/E model values are also in close agreement with the polarizable models, suggesting that the effective treatment of water molecule polarization may be considered reasonably justified even for the cluster cation systems. However, even though the model predictions are mutually similar, they all fail to reproduce the

trends seen in the experimental results. In particular, the simulated dependence of $\Delta H^{\circ}_{n-1,n}$ for n = 1 to 5 is convex (bends upward), whereas the experimentally determined dependence is concave, which leads to large deviations for midsize clusters. For instance, $\Delta H^{\circ}_{2,3}\left[\mathrm{Na}^{+}\right]$ differs by as much as ~10 kJ/mol for the most accurate model included in the comparison. Moreover, the simulation results exhibit a sharp change in their trend at n = 5, a behavior not observed in experiments.

It is not immediately clear why the above models deviate from the experimental results. In fact, similar discrepancies between the experiment and a simple electrostatic model were noted and discussed in the original paper by Dzidic and Kebarle,[13] who suggested that some form of covalency may be missing from the interaction model. To test this hypothesis, we have plotted in Figure 4 a comparison between the model descriptions and our quantum chemical simulation results for the hydration enthalpies, from which we can observe an obvious resemblance between quantum outcome and the classical models. Moreover, our preliminary simulations with the popular AMOEBA force field yielded a similar convex dependence for $\Delta H^{\circ}_{n-1,n}\left[\mathrm{Li}^{+}\right]$ and $\Delta H^{\circ}_{n-1,n}\left[\mathrm{Na}^{+}\right]$ in close agreement with the quantum chemical results. The latest outcome pushes the issue about a plausible explanation behind the observed discrepancies, including the assumptions built into the experimental method, which involves extrapolations from high temperature measurements to 298.15 K, and the neglected or underrepresented ion-water interactions, such as charge transfer effects,[77] in the computational models. In support to the last contention, an alternative set of data for the enthalpies of Na^{+} hydration (n = 1-4) at 0 K based on the collision-induced dissociation experiments appear more consistent with the classical and quantum simulation results than those from the HPMS experiments.[16]

The analysis of the cluster structural properties can facilitate the microscopic interpretation of the observed hydration thermodynamics, as illustrated in Figure 5 where we compare the ion-oxygen pair distribution functions for Li^+ and Na^+ clusters with n = 1 and 5, as predicted by the classical models, and DFT calculations. The main distinctive feature in this comparison is the shift to shorter separations of the first peak of the BK3 distribution functions. Interestingly, the DFT data are most closely matched by the SPC/E model.

In terms of the incremental hydration Gibbs free energies of halide anions, Figure 6 displays the evolution of $\Delta G^{\circ}_{n-1,n}$ where we can observe that the overall agreement of modeling results with experimental data is poorer than for alkaline cations. The largest discrepancies are seen for the SPC/E-based model of small F^- clusters even when the polarization correction is included. The SWM4-DP model predictions also deviate significantly for the lowest values of n, where they are still noticeable for heavier halide ions, though gradually decreasing. The BK3 model predictions are nearly in quantitative agreement for F^- systems, but the model's performance deteriorates with the increasing atomic weight of the halide ion. A likely explanation for the satisfactory description of the F^- clusters by the BK3 model lies in its use of three polarizable sites, two of which are located at the hydrogens. As discussed in the early work by Arshadi and co-workers,[78] the large negative energy of the first stepwise hydration reaction, $F^- + H_2O \rightarrow F^-(H_2O)$ may be caused by the partial charge and proton transfer in the strong hydrogen bond $F^- \ldots H^+ \ldots OH^-$ (see Figure 7). While the current rigid non-reactive models cannot accurately reproduce such interactions, the charge-on-spring hydrogen of the BK3 model can emulate their effects. This is not possible for the SPC/E and SWM4-DP representations, consequently, they fail to reproduce the hydration trends not only for the F^- clusters but also for the remaining halides. A systematic investigation of the SPC/E-based alkali halide models confirms that the

observed discrepancies between model predictions and HPMS do not come from the model's parametrization but from its functional form, and that the unsatisfactory reproduction of anion-water interactions extends to the bulk solution properties.[19]

The behavior of $\Delta H^{\circ}_{n-1,n}$ for halide anions illustrated in Figure 8 demonstrates that a reasonable prediction of hydration free energies does not guarantee correct enthalpies (or entropies for that matter). While the discrepancies in the SPC/E and SWM4-DP model predictions are qualitatively the same as in the case of $\Delta G^{\circ}_{n-1,n}$, an unexpected behavior is exhibited by the BK3 model for $\Delta H^{\circ}_{2,3}\left[X^{-}\right]$, where X = Cl, Br or, I. Unlike the experimental or other model description including the AMOEBA force field,[33] the BK3 model predicts a sharply lower enthalpy when adding the third water molecule to the cluster. A closer look at the generated low energy structures reveals the formation of a symmetric pyramidal structure as depicted in Figure 9. The relative stability of this configuration was observed in quantum chemical calculations for all halide ions,[79,80] but it is clearly exaggerated by the BK3 model, an artifact that illustrates the challenges underlying the development of accurate molecular models and the need for their thorough testing.

Finally, in Figure 10 we compare the ion-oxygen and ion-hydrogen pair distribution functions for selected F^- clusters predicted by classical and *ab initio* simulations, where we observe, as in the case of Li^+ and Na^+ ions (Figure 5), that the peaks of the BK3 model distribution functions are shifted to shorter separations compared to both the SPC/E and quantum results. The shorter H_2O - F^- distances may be required to compensate for the decreased ion-hydrogen attraction resulting from the overlapping Gaussian charges.

4. Conclusions

We have tested the ability of classical molecular models to describe the microstructural and thermodynamic behavior of gas-phase hydration of alkali halides clusters and the formation of small water clusters, through the interrogation of the effect of many-body interactions (polarization) and charge penetration on determining the incremental hydration Gibbs free energy and corresponding enthalpy. For that purpose we employed three contrasting models including (i) point charge non-polarizable SPC/E, (ii) Drude point charge polarizable SWM4-DP, and (iii) Drude Gaussian charge polarizable BK3.

We have performed a series of classical and quantum chemical simulations of gas phase ion hydration at 298.15 K to assess the performance of force field parameterizations of the above models. Even though it is not always possible to distinguish between the failings of a specific parametrization from the deficiencies of the interaction model itself, the resulting extensive data sets and the analysis of hydration trends allowed us to draw more general conclusions about the factors controlling the ion hydration process while simultaneously raising questions about the accuracy of the available experimental data.

In general, the investigated classical models are able to describe alkali cationic clusters more accurately than the halide anionic counterparts. Even though there is a significant disagreement between the experimental Na^+ hydration enthalpies of Dzidic and Kebarle[13] and the corresponding modeling results based on quantum chemical or classical simulations, it appears that even very simple non-polarizable models using point charges and Lennard-Jones interactions can capture the essence of the cation-water interactions. Water-anion interactions involving the formation of strong hydrogen bonds appear as a more complex hydration process that requires incorporation of many-body effects. Our analysis of the SWM4-DP and BK3 polarizable models suggests that a single polarizable site located at, or near, the oxygen center

may not be sufficient to reproduce the hydration thermodynamic trends seen in experimental data, which was only achievable through additional polarizable sites located at the hydrogen atoms, as in the case of BK3 and AMOEBA force fields. As we might have expected, the overall agreement between model predictions and experimental data improves with increasing model complexity. However, even adequate description of the hydration thermodynamics does not guarantee overall agreement of the cluster ion structural properties, as highlighted by the example of the BK3 model description of $Cl^-(H_2O)_3$ clusters.

The combination of classical and quantum chemical simulations, together with the alternative CID experiments, indicate that there might be underlying inaccuracies in the high-pressure mass spectrometry determination of small cation hydration. While the present study cannot conclusively answer this question, or pinpoint their sources, it highlights issues that will have to be resolved in order to develop and validate predictively accurate models of ion-water interactions.

ACKNOWLEDGMENT

Research supported by the Division of Chemical Sciences, Geosciences, and Biosciences, Office of Basic Energy Sciences, U.S. Department of Energy. The participation of F.M. and I.N. was facilitated by the Czech-USA cooperative research program "Nonadditive interactions in aqueous solutions of electrolytes". F. U. thanks the Czech Science Foundation (P208/10/1724) and access to the CERIT-SC computing facilities (CZ.1.05/3.2.00/08.0144)

References

(1) Ferguson, E. E. *Mass Spectrom. Rev.* **2007**, *26*, 142.

(2) Ghosal, S.; Hemminger, J. C.; Bluhm, H.; Mun, B. S.; Hebenstreit, E. L. D.; Ketteler, G.; Ogletree, D. F.; Requejo, F. G.; Salmeron, M. *Science* **2005**, *307*, 563.

(3) Hayhurst, A. N.; Sugden, T. M. *Proceedings of the Royal Society of London Series a-Mathematical and Physical Sciences* **1966**, *293*, 36.

(4) Hayhurst, A. N. *Combustion Explosion and Shock Waves* **2012**, *48*, 516.

(5) Hvelplund, P.; Pedersen, J. O. P.; Stochkel, K.; Enghoff, M. B.; Kurten, T. *International Journal of Mass Spectrometry* **2013**, *341*, 1.

(6) Pitzer, K. S.; Palaban, R. T. *Geochemica et Cosmochimica Acta* **1986**, *50*, 1445.

(7) Chialvo, A. A.; Gruszkiewicz, M. S.; Cole, D. R. *Journal of Chemical & Engineering Data* **2010**, *55*, 1828.

(8) Kebarle, P.; Verkerk, U. H. *Mass Spectrom. Rev.* **2009**, *28*, 898.

(9) Payzant, J. D.; Yamdagni, R.; Kebarle, P. *Canadian Journal of Chemistry* **1971**, *49*, 3308.

(10) Blades, A. T.; Kebarle, P. *J. Phys. Chem. A* **2005**, *109*, 8293.

(11) Blades, A. T.; Jayaweera, P.; Ikonomou, M. G.; Kebarle, P. *International Journal of Mass Spectrometry and Ion Processes* **1990**, *102*, 251.

(12) Blades, A. T.; Peschke, M.; Verkerk, U. H.; Kebarle, P. *J. Am. Chem. Soc.* **2004**, *126*, 11995.

(13) Dzidic, I.; Kebarle, P. *J. Phys. Chem.* **1970**, *74*, 1466.

(14) Hiraoka, K.; Mizuse, S.; Yamabe, S. *J. Phys. Chem.* **1988**, *92*, 3943.

(15) Amicangelo, J. C.; Armentrout, P. B. *J. Phys. Chem. A* **2004**, *108*, 10698.

(16) Dalleska, N. F.; Tjelta, B. L.; Armentrout, P. B. *J. Phys. Chem.* **1994**, *98*, 4191.

(17) Rodgers, M. T.; Armentrout, P. B. *J. Phys. Chem. A* **1997**, *101*, 1238.

(18) Tissandier, M. D.; Cowen, K. A.; Feng, W. Y.; Gundlach, E.; Cohen, M. H.; Earhart, A. D.; Coe, J. V.; Tuttle, T. R. *J. Phys. Chem. A* **1998**, *102*, 7787.

(19) Vlcek, L.; Chialvo, A. A.; Simonson, J. M. *J. Phys. Chem. A* **2013**, *117*, 11328.

(20) Lukyanov, S. I.; Zidi, Z. S.; Shevkunov, S. V. *Chemical Physics* **2007**, *332*, 188.

(21) Shevkunov, S. V. *Colloid J.* **2009**, *71*, 406.

(22) Ren, P. Y.; Ponder, J. W. *J. Phys. Chem. B* **2003**, *107*, 5933.

(23) Joung, I. S.; Cheatham, T. E. *J. Phys. Chem. B* **2008**, *112*, 9020.

(24) Lamoureux, G.; Roux, B. *J. Phys. Chem. B* **2006**, *110*, 3308.

(25) Dang, L. X. *J. Chem. Phys.* **1999**, *110*, 1526.

(26) Bako, I.; Hutter, J.; Palinkas, G. *J. Chem. Phys.* **2002**, *117*, 9838.

(27) McGrath, M. J.; Kuo, I. F. W.; Ngouana W, B. F.; Ghogomu, J. N.; Mundy, C. J.; Marenich, A. V.; Cramer, C. J.; Truhlar, D. G.; Siepmann, J. I. *Phys. Chem. Chem. Phys.* **2013**, *15*, 13578.

(28) Baranyai, A.; Kiss, P. T. *The Journal of Chemical Physics* **2010**, *133*, 144109.

(29) Fanourgakis, G. S.; Xantheas, S. S. *J. Phys. Chem. A* **2006**, *110*, 4100.

(30) Paricaud, P.; Predota, M.; Chialvo, A. A.; Cummings, P. T. *J. Chem. Phys.* **2005**, *122*.

(31) Yu, H. B.; van Gunsteren, W. F. *J. Chem. Phys.* **2004**, *121*, 9549.

(32) Dang, L. X.; Chang, T. M. *J. Chem. Phys.* **1997**, *106*, 8149.

(33) Grossfield, A.; Ren, P. Y.; Ponder, J. W. *J. Am. Chem. Soc.* **2003**, *125*, 15671.

(34) Dang, L. X.; Rice, J. E.; Caldwell, J.; Kollman, P. A. *J. Am. Chem. Soc.* **1991**, *113*, 2481.

(35) Smith, D. E.; Dang, L. X. *J. Chem. Phys.* **1994**, *101*, 7873.

(36) Smith, D. E.; Dang, L. X. *J. Chem. Phys.* **1994**, *100*, 3757.
(37) Shevkunov, S. V. *Colloid J.* **2010**, *72*, 93.
(38) Zidi, Z. S. *J. Chem. Phys.* **2012**, *137*, 124107.
(39) Galashev, A. Y. *Can. J. Chem.-Rev. Can. Chim.* **2011**, *89*, 524.
(40) Brodskaya, E.; Lyubartsev, A. P.; Laaksonen, A. *J. Chem. Phys.* **2002**, *116*, 7879.
(41) Darden, T.; Pearlman, D.; Pedersen, L. G. *J. Chem. Phys.* **1998**, *109*, 10921.
(42) Kelly, C. P.; Cramer, C. J.; Truhlar, D. G. *J. Phys. Chem. B* **2006**, *110*, 16066.
(43) Tuttle, T. R.; Malaxos, S.; Coe, J. V. *J. Phys. Chem. A* **2002**, *106*, 925.
(44) Pollard, T.; Beck, T. L. *J. Chem. Phys.* **2014**, *140*, 11.
(45) Ferrenberg, A. M.; Swendsen, R. H. *Phys. Rev. Lett.* **1989**, *63*, 1195.
(46) Bennett, C. H. *J. Comput. Phys.* **1976**, *22*, 245.
(47) Hansen, J. P.; McDonald, I. R. *Theory of Simple Liquids*; 3rd ed.; Academic Press: Amsterdam, 2006.
(48) Widom, B. *J. Chem. Phys.* **1963**, *39*, 2808.
(49) Schenter, G. K. *J. Chem. Phys.* **1998**, *108*, 6222.
(50) Stoddard, S. D. *J. Comput. Phys.* **1978**, *27*, 291.
(51) Lukyanov, S. I.; Zidi, Z. S.; Shevkunov, S. *Journal of Molecular Structure-Theochem* **2005**, *725*, 191.
(52) Hill, T. L. *J. Chem. Phys.* **1955**, *23*, 617.
(53) Hill, T. L. *J. Chem. Phys.* **1955**, *23*, 623.
(54) Pugnaloni, L. A.; Zarragoicoechea, G. J.; Vericat, F. *J. Chem. Phys.* **2006**, *125*, 10.
(55) Skvor, J.; Nezbeda, I. *Mol. Phys.* **2011**, *109*, 133.
(56) Berendsen, H. J. C.; Grigera, J. R.; Straatsma, T. P. *J. Phys. Chem.* **1987**, *91*, 6269.
(57) Lamoureux, G.; MacKerell, A. D.; Roux, B. *J. Chem. Phys.* **2003**, *119*, 5185.
(58) Kiss, P. T.; Baranyai, A. *J. Chem. Phys.* **2013**, *138*, 17.
(59) Norman, G. E.; Filinov, V. S. *High Temp.* **1969**, *7*, 216.
(60) Moucka, F.; Nezbeda, I.; Smith, W. R. *Molecular Simulation* **2013**, *39*, 1125.
(61) Paesani, F.; Iuchi, S.; Voth, G. A. *J. Chem. Phys.* **2007**, *127*, 15.
(62) Chai, J. D.; Head-Gordon, M. *Phys. Chem. Chem. Phys.* **2008**, *10*, 6615.
(63) Leverentz, H. R.; Qi, H. W.; Truhlar, D. G. *J. Chem. Theory Comput.* **2013**, *9*, 995.
(64) Dunning, T. H. *J. Chem. Phys.* **1989**, *90*, 1007.
(65) Frisch, M. J.; Trucks, G. W.; Schlegel, H. B.; Scuseria, G. E.; Robb, M. A.; Cheeseman, J. R.; Scalmani, G.; Barone, V.; Mennucci, B.; Petersson, G. A.; Nakatsuji, H.; Caricato, M.; Li, X.; Hratchian, H. P.; Izmaylov, A. F.; Bloino, J.; Zheng, G.; Sonnenberg, J. L.; Hada, M.; Ehara, M.; Toyota, K.; Fukuda, R.; Hasegawa, J.; Ishida, M.; Nakajima, T.; Honda, Y.; Kitao, O.; Nakai, H.; Vreven, T.; Montgomery Jr., J. A.; Peralta, J. E.; Ogliaro, F.; Bearpark, M. J.; Heyd, J.; Brothers, E. N.; Kudin, K. N.; Staroverov, V. N.; Kobayashi, R.; Normand, J.; Raghavachari, K.; Rendell, A. P.; Burant, J. C.; Iyengar, S. S.; Tomasi, J.; Cossi, M.; Rega, N.; Millam, N. J.; Klene, M.; Knox, J. E.; Cross, J. B.; Bakken, V.; Adamo, C.; Jaramillo, J.; Gomperts, R.; Stratmann, R. E.; Yazyev, O.; Austin, A. J.; Cammi, R.; Pomelli, C.; Ochterski, J. W.; Martin, R. L.; Morokuma, K.; Zakrzewski, V. G.; Voth, G. A.; Salvador, P.; Dannenberg, J. J.; Dapprich, S.; Daniels, A. D.; Farkas, Ö.; Foresman, J. B.; Ortiz, J. V.; Cioslowski, J.; Fox, D. J.; Gaussian, Inc.: Wallingford, CT, USA, 2009.

(66) Gelb, L. D. *J. Chem. Phys.* **2003**, *118*, 7747.
(67) Toukan, K.; Rahman, A. *Physical Review B* **1985**, *31*, 2643.
(68) Lee, S. H.; Rasaiah, J. C. *J. Phys. Chem.* **1996**, *100*, 1420.
(69) Kell, G. S.; McLaurin, G. E. *J. Chem. Phys.* **1969**, *51*, 4345.
(70) Kell, G. S.; McLaurin, G. E.; Whalley, E. *J. Chem. Phys.* **1968**, *48*, 3805.
(71) Coe, J. V. *Chem. Phys. Lett.* **1994**, *229*, 161.
(72) Buffey, I. P.; Brown, W. B. *Chem. Phys. Lett.* **1984**, *109*, 59.
(73) Shields, R. M.; Temelso, B.; Archer, K. A.; Morrell, T. E.; Shields, G. C. *J. Phys. Chem. A* **2010**, *114*, 11725.
(74) Kiss, P. T.; Baranyai, A. *J. Chem. Phys.* **2009**, *131*, 14.
(75) Habershon, S. *Phys. Chem. Chem. Phys.* **2014**, *16*, 9154.
(76) Vlcek, L.; Chialvo, A. A., manuscript in preparation
(77) Soniat, M.; Rick, S. W. *J. Chem. Phys.* **2012**, *137*, 9.
(78) Arshadi, M.; Yamdagni, R.; Kebarle, P. *J. Phys. Chem.* **1970**, *74*, 1475.
(79) Gora, R. W.; Roszak, S.; Leszczynski, J. *Chem. Phys. Lett.* **2000**, *325*, 7.
(80) Xantheas, S. S. *J. Phys. Chem.* **1996**, *100*, 9703.

Figure captions

Figure 1: Incremental hydration Gibbs free energies (top) and enthalpies (bottom) of pure water clusters. Experiment[69,70] (black), SPC/E (blue – filled circles), polarization corrected SPC/E (blue – open circles), SWM4-DP (green), BK3 (red), and MP2-level *ab initio*[73] (magenta).

Figure 2: Oxygen-oxygen pair distribution functions for BK3 water clusters, n = 2 to 6.

Figure 3: Incremental hydration Gibbs free energies of alkali metal ions. HPMS experiment[13] (black), SPC/E (blue – filled circles), polarization corrected SPC/E (blue – open circles), SWM4-DP (green), and BK3 (red).

Figure 4: Incremental hydration enthalpies of alkali metal ions. HPMS experiment[13] (black – filled circles), CID experiment[16,17] (black - open circles), SPC/E (blue – filled circles), polarization corrected SPC/E (blue – open circles), SWM4-DP (green), BK3 (red).), and DFT (magenta).

Figure 5: Ion-oxygen pair distribution functions for Li^+ (left) Na^+ (right) cluster ions with n = 1 (top) and n = 5 (bottom) predicted by SPC/E (blue), SWM4-DP (green), and BK3 (red) models and DFT potential (black).

Figure 6: Incremental hydration Gibbs free energies of halide ions. HPMS experiment[14] (black), SPC/E (blue – filled circles), polarization corrected SPC/E (blue – open circles), SWM4-DP (green), and BK3 (red).

Figure 7: Electrostatic potential around an F^- - H_2O dimer in atomic units (a.u.) at the contour of electronic density of 0.05 a.u.

Figure 8: Incremental hydration enthalpies of halide ions. HPMS experiment[14] (black – filled circles), SPC/E (blue – filled circles), polarization corrected SPC/E (blue – open circles), SWM4-DP (green), BK3 (red).), and DFT (magenta).

Figure 9: Side (left) and top (right) view of the stable pyramidal structure formed by BK3 $Cl^-(H_2O)_3$ clusters.

Figure 10: Ion-oxygen (left) and ion-hydrogen (right) pair distribution functions for F^- clusters with $n = 1$ (top) and $n = 5$ (bottom) predicted by the SPC/E (blue), SWM4-DP (green), and BK3 (red) models and DFT potential (black).

Figure 1

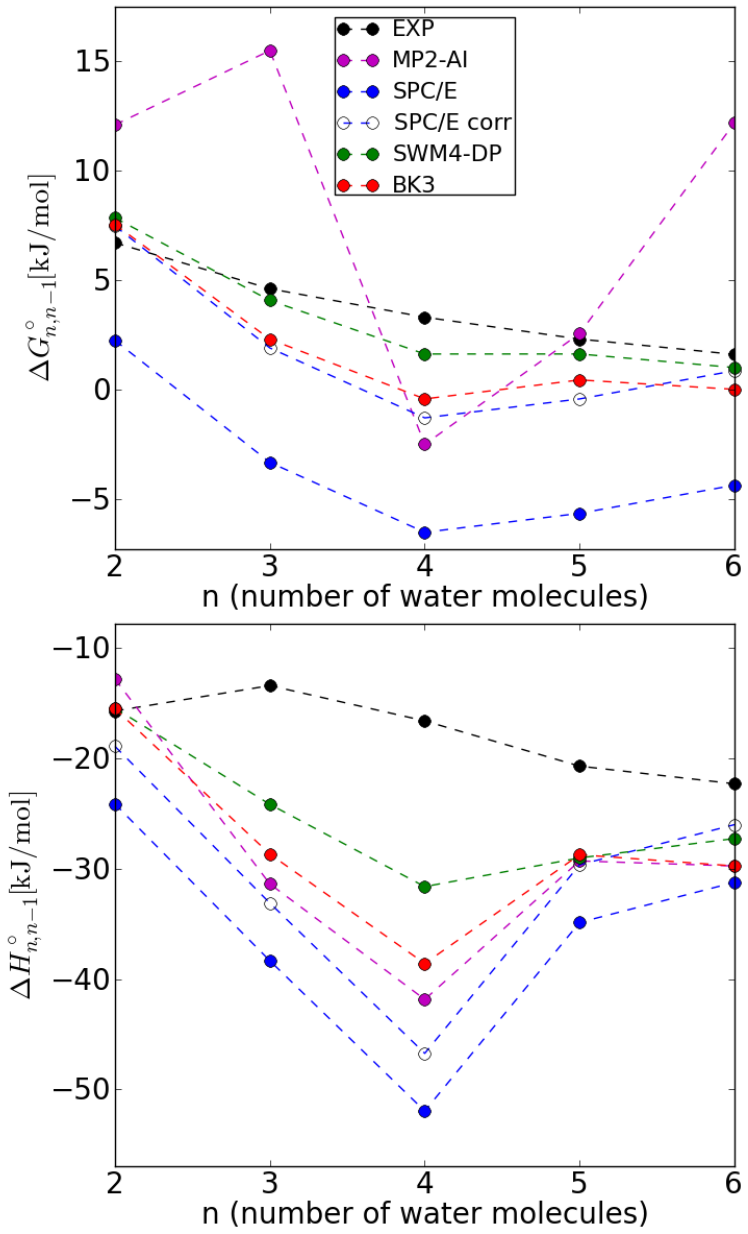
EXP
MP2-AI
SPC/E
SPC/E corr
SWM4-DP
BK3
$\Delta G^{\circ}_{n,n-1}$[kJ/mol]
n (number of water molecules)
$\Delta H^{\circ}_{n,n-1}$[kJ/mol]
n (number of water molecules)

Figure 2

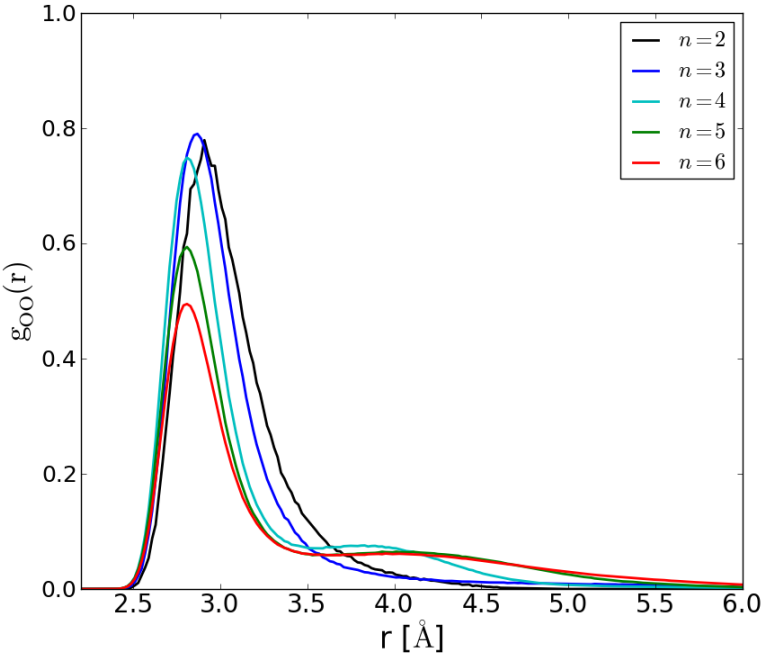

Figure 3

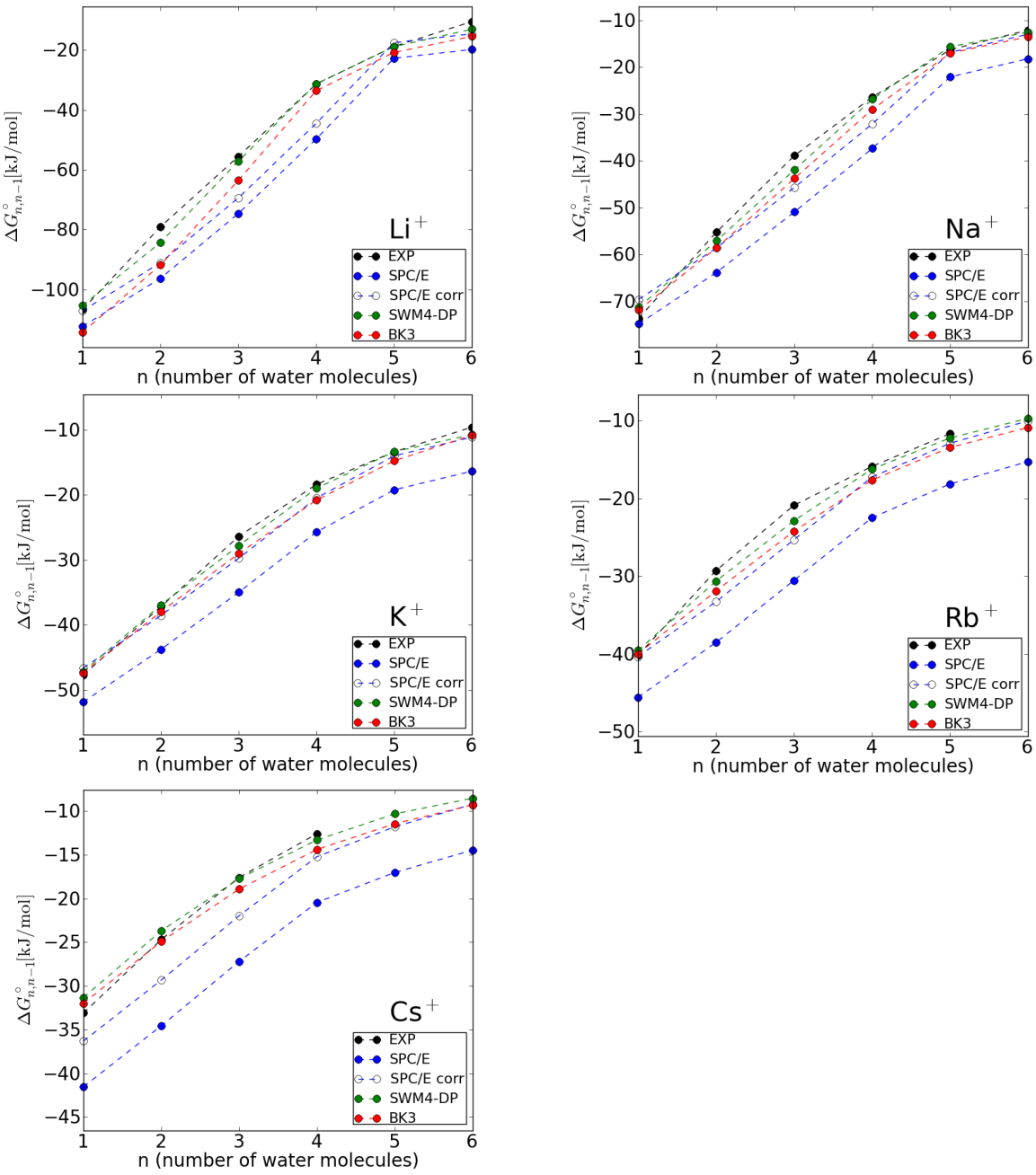
Li+
Na+
K+
Rb+
Cs+
EXP
SPC/E
SPC/E corr
SWM4-DP
BK3
n (number of water molecules)
$\Delta G^{\circ}_{n,n-1}$[kJ/mol]

Figure 4

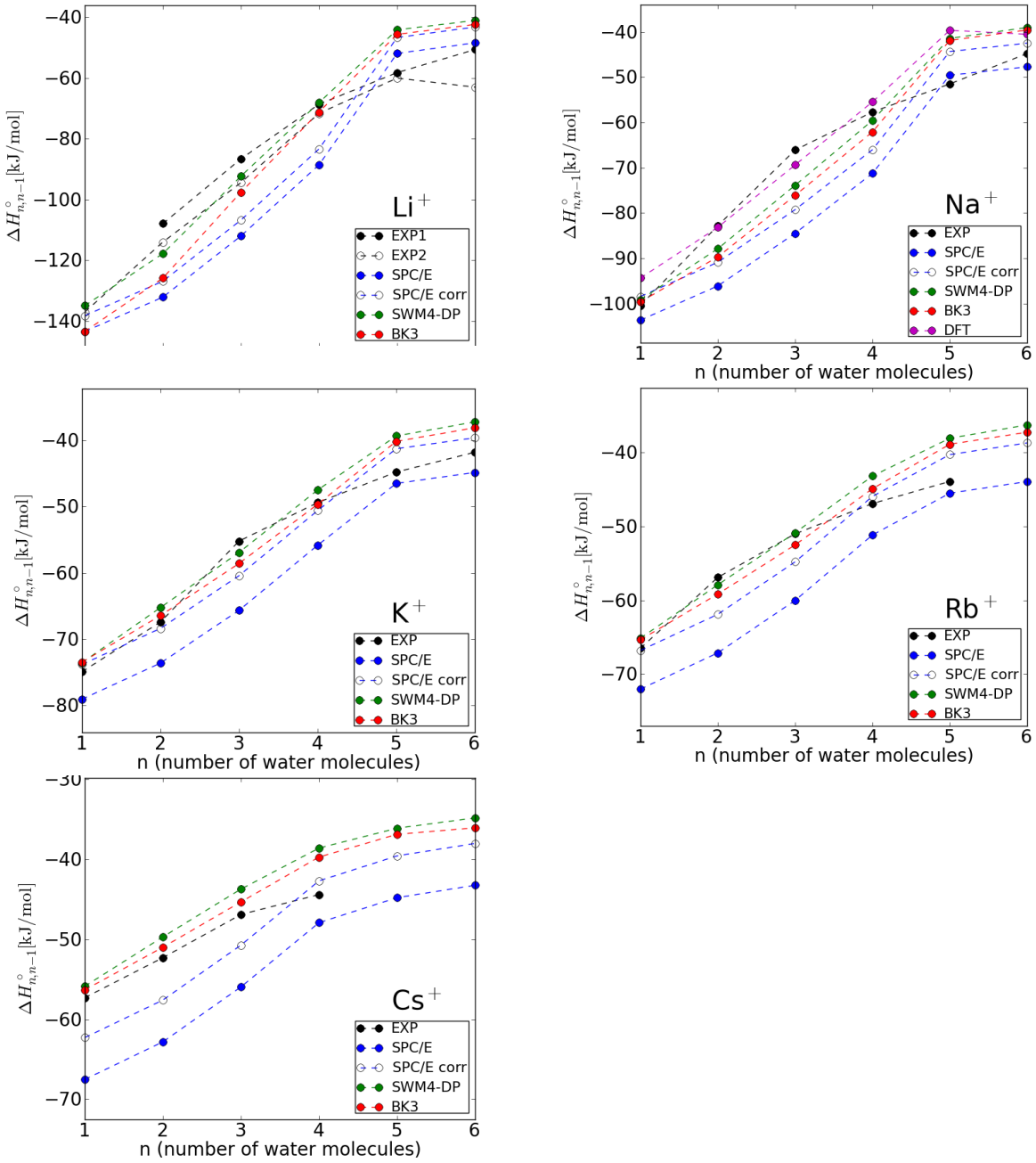
$\Delta H^{\circ}_{n,n-1}$[kJ/mol]
n (number of water molecules)
Li$^+$
EXP1
EXP2
SPC/E
SPC/E corr
SWM4-DP
BK3
Na$^+$
EXP
SPC/E
SPC/E corr
SWM4-DP
BK3
DFT
K$^+$
EXP
SPC/E
SPC/E corr
SWM4-DP
BK3
Rb$^+$
EXP
SPC/E
SPC/E corr
SWM4-DP
BK3
Cs$^+$
EXP
SPC/E
SPC/E corr
SWM4-DP
BK3

Figure 5

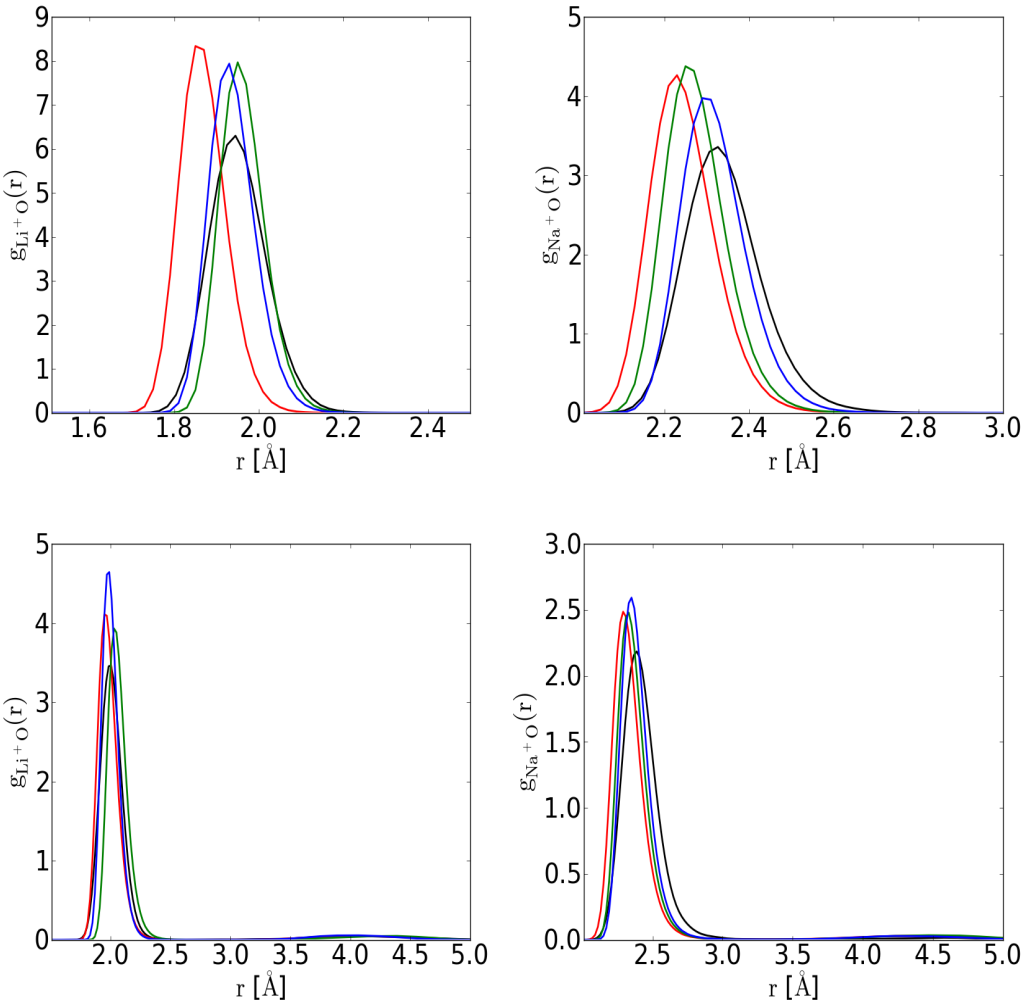

Figure 6

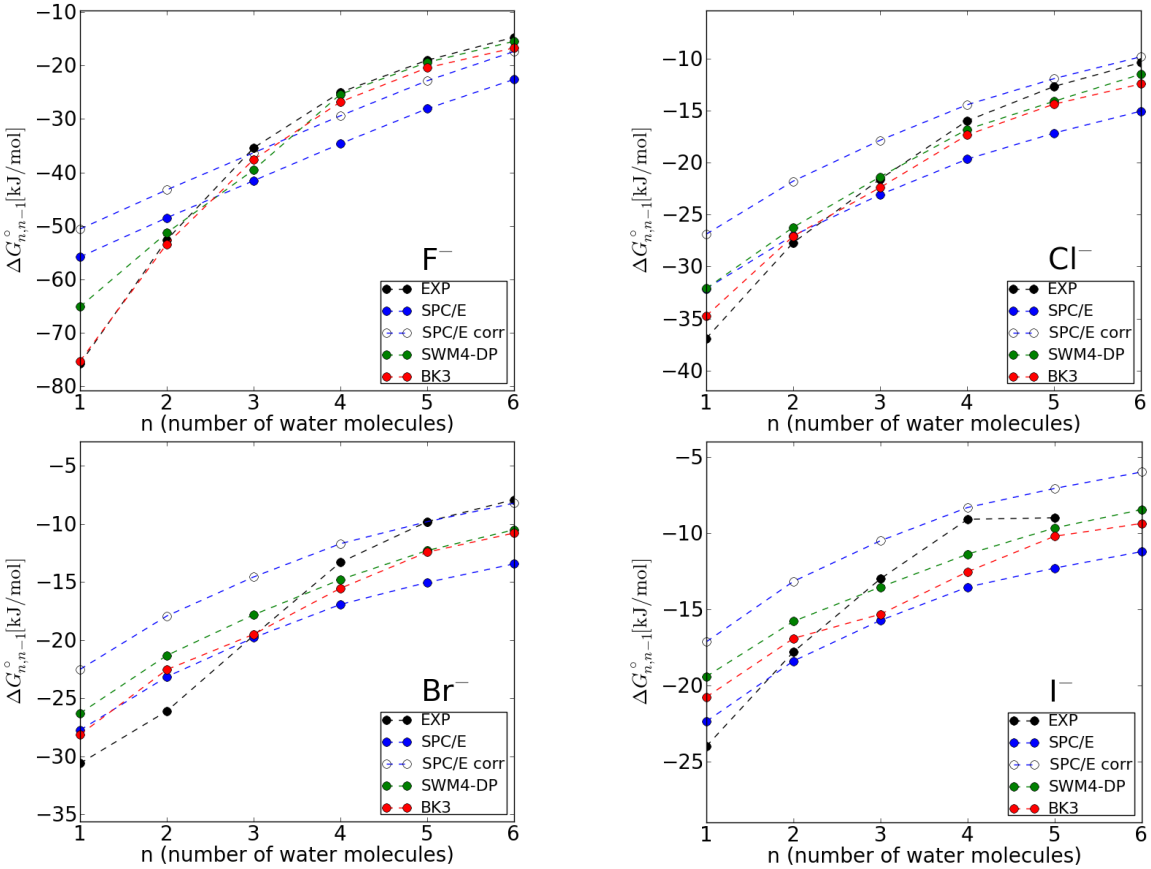
F⁻
Cl⁻
Br⁻
I⁻
EXP
SPC/E
SPC/E corr
SWM4-DP
BK3
n (number of water molecules)
$\Delta G^{\circ}_{n,n-1}$[kJ/mol]

Figure 7

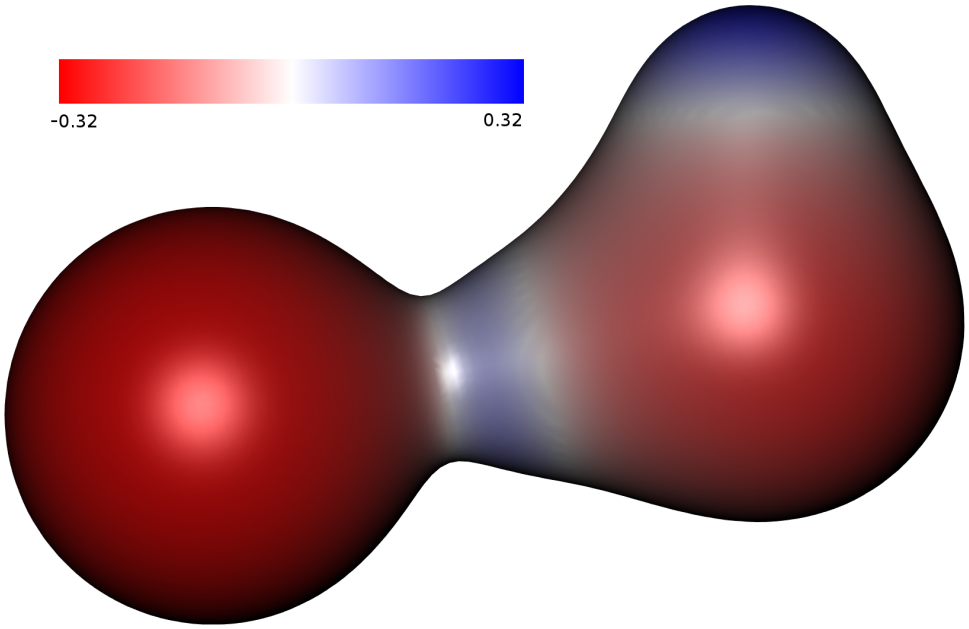

Figure 8

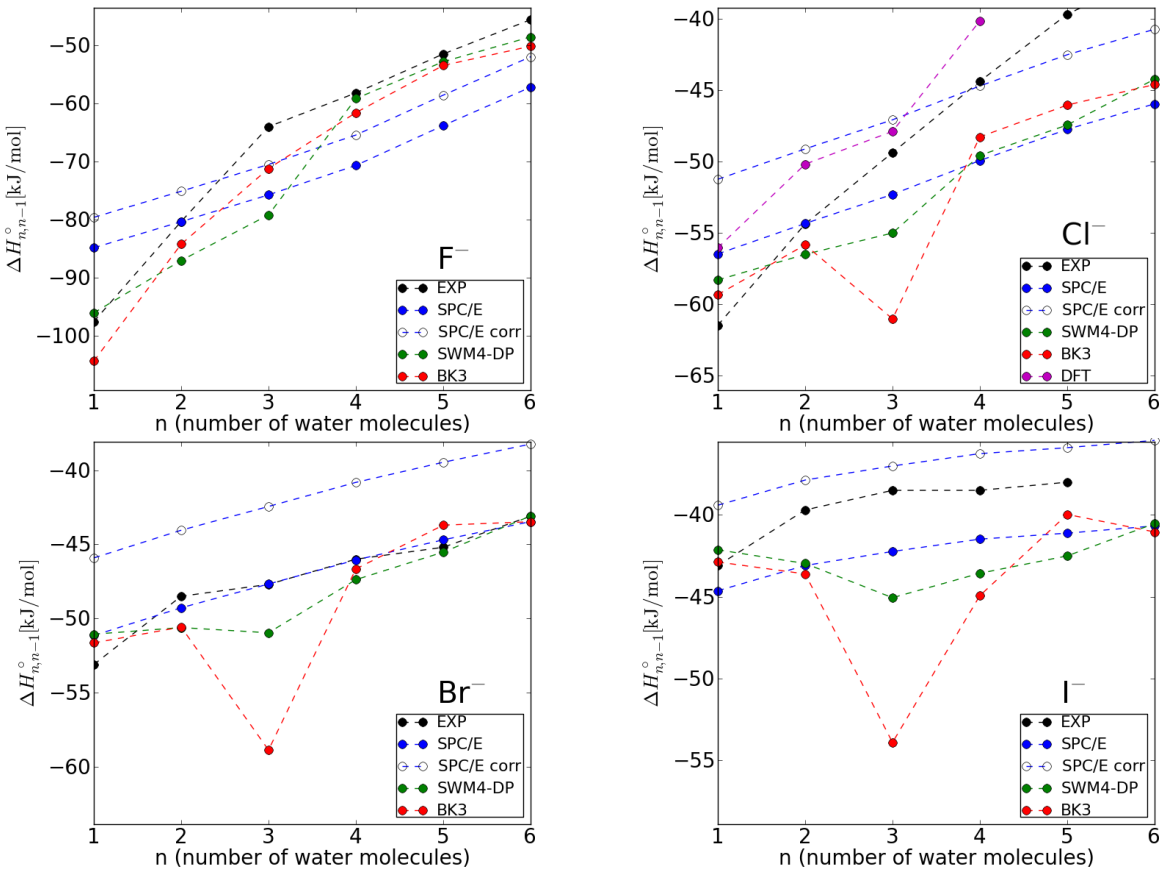
F⁻
Cl⁻
Br⁻
I⁻
EXP
SPC/E
SPC/E corr
SWM4-DP
BK3
DFT
n (number of water molecules)
$\Delta H^{\circ}_{n,n-1}$[kJ/mol]

Figure 9

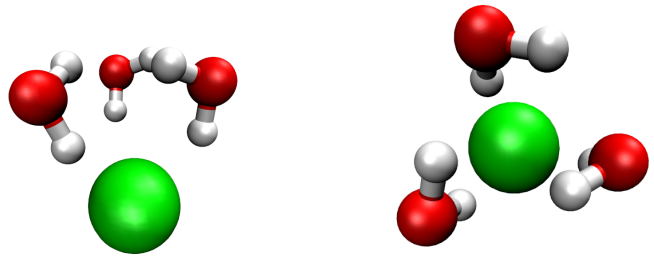

Figure 10